

Article

Bayesian modelling of longitudinal data with space-time interaction and bootstrap analysis

Aliyu Abba Mustapha^{1*}, Hani Syahida Zulkafli², Jayanthi Arasan³, and Mohammed Abba Mustapha⁴

¹ Department of Mathematics and Statistics, Universiti Putra Malaysia, 43400 UPM Serdang, Selangor, Malaysia; gs61204@student.upm.edu.my

² Department of Mathematics and Statistics, Universiti Putra Malaysia, 43400 UPM Serdang, Selangor, Malaysia; hsyahida@upm.edu.my

³ Department of Mathematics and Statistics, Universiti Putra Malaysia, 43400 UPM Serdang, Selangor, Malaysia; jayanthi@upm.edu.my

⁴ World Health Organization, Borno State Field Office, Maiduguri, Nigeria; abbamusthydr@gmail.com

* Correspondence: gs61204@student.upm.edu.my; <https://orcid.org/0000-0002-6445-0831>

Abstract: This paper presents a Bayesian spatio-temporal model with space-time interaction effects for longitudinal data. The main objective is to evaluate how spatial and temporal dependencies, together with their interactions, influence parameter estimation and interpretation. The model incorporates spatial random effects to capture unobserved heterogeneity between neighboring regions, temporal random effects to reflect trends over time, and interaction terms to account for localized space-time variations. A conditional autoregressive (CAR) prior is applied to address spatial dependence, while Markov chain Monte Carlo (MCMC) sampling is used for posterior estimation, supported by convergence diagnostics such as trace plots and the Geweke test. Bootstrap analysis is also applied to assess the stability of estimates and provide complementary validation. Results based on simulated datasets across multiple areal unit sizes show that the intercept and covariate effects are sensitive to spatial resolution, whereas spatial and temporal correlations remain relatively stable across scales. The variance components, particularly the interaction term, capture localized heterogeneity more effectively at smaller spatial units. The findings demonstrate that combining Bayesian estimation with bootstrap analysis provides a reliable framework for understanding spatial and temporal disease dynamics, with practical implications for public health planning and intervention strategies.

Keywords: Bayesian spatio-temporal model, spatial effect, temporal effect, interaction effect, hierarchical Bayesian modeling, bootstrap analysis.

Received: 6 December 2025; Revised: 15 January 2026; Accepted: 22 January 2026; Published: 5 February 2026



Copyright: ©2026 the Author(s). Published by JSSCI. This is an open-access article distributed under the terms of the Creative Commons Attribution 4.0 International License (CC BY 4.0).

Journal Abbreviation: J. Stat. Sci. Comput. Intell.

1. Introduction

Understanding the dynamics of longitudinal data is a central challenge in modern statistical modelling, particularly when the data exhibit both spatial and temporal dependencies. Longitudinal datasets often involve repeated observations collected from multiple units over time, where correlations exist not only across time within the same unit but also cross space between different units. For instance, in epidemiological research, disease incidence recorded repeatedly across areas and time periods may display nontrivial dependencies that cannot be adequately captured by classical approaches. Ignoring such dependencies can lead to biased estimates, underestimated uncertainty, and misleading inference. As the scale complexity of longitudinal data increase, there is a pressing need for flexible statistical frameworks that can model space-time interactions while simultaneously providing reliable mechanisms for uncertainty quantification.

Exploring the dynamics of longitudinal data across both spatial and temporal dimensions is essential for accurately characterizing complex real-world phenomena [9, 3,16]. Such data structures arise in diverse fields including epidemiology, environmental science, public health, and socio-economic studies, where repeated measurements are collected over time and across distinct geographical units. Conventional analytical approaches often treat space and time independently, thereby overlooking the intricate interplay between spatial heterogeneity and temporal evolution. This separation limits their ability to detect joint patterns, which are crucial for identifying localized temporal trends, assessing intervention impacts, and forecasting outcomes in dynamic environments.

The increasing availability of high-resolution spatio-temporal datasets enabled by advances in sensing technologies, remote monitoring systems, and real-time data reporting has expanded opportunities for in-depth longitudinal analysis. However, these data also present challenges due to their complexity, size, and the presence of multiple sources of variability. Bayesian hierarchical modeling has emerged as a powerful framework for addressing these challenges, offering a coherent way to integrate spatial and temporal dependencies, incorporate prior knowledge, and quantify uncertainty in both parameters and predictions [14, 6].

Building on these developments, spatio-temporal modelling provides a structured approach to investigate phenomena that vary across both space and time. Bayesian hierarchical binomial logistic regression offers a flexible framework that incorporates spatial, temporal, and space-time interaction effects, facilitating comprehensive analysis of binary outcomes [20]. In such models, the inclusion of space, time, and their interaction is essential for capturing the complex dynamics of the phenomenon being investigated. Spatial random effects address unobserved spatial heterogeneity and spatial autocorrelation, temporal random effects capture dependencies and trends over time, and interaction terms allow covariate–outcome relationships to vary jointly across space and time [12]. This combination ensures that parameter estimation accounts for both localized spatial variation and temporal evolution, providing a richer picture of the processes under study.

The foundational work of [5] introduced Bayesian hierarchical spatio-temporal models for disease risk, accounting for both spatial and temporal effects along with their interactions. Subsequent methodological advances have improved computational efficiency and scalability. For example, [8] proposed fixed rank kriging for handling large spatial datasets in spatio-temporal models. More recently, Gaussian process priors and scalable approximations have been introduced to efficiently capture complex dependencies while managing computational costs. With the growing availability of high-resolution spatio-temporal data, Bayesian hierarchical modelling has gained prominence due to its ability to incorporate uncertainty and variability at multiple levels of the model [20].

Bayesian hierarchical binomial logistic regression, which integrates spatial, temporal, and space-time

interaction effects, has been applied widely across epidemiology, ecology, and socio-demographic studies. For example, [11] and later applications by [21] demonstrated the value of Bayesian inference in understanding spatial and temporal patterns of infectious disease transmission. In contrast to frequentist approaches, which assume parameters are fixed but unknown, Bayesian methods treat parameters as random variables represented by probability distributions. This framework enables richer inference, allowing researchers to quantify parameter uncertainty while borrowing strength across neighboring areal units and adjacent time periods [15, 19].

The integration of bootstrap analysis further enhances this framework by providing an empirical means to assess the robustness and stability of parameter estimates, offering additional insights into model uncertainty. Although Bayesian posterior distributions already quantify uncertainty, bootstrap validation serves as an independent check, particularly in small samples or highly heterogeneous contexts. Bootstrap-based resampling helps ensure that findings are not artifacts of prior assumptions or sampling variability, thereby reinforcing the reliability of conclusions [7, 1].

Applied to longitudinal data, this Bayesian space-time interaction approach allows for detailed understanding of complex dynamics, capturing localized variations and temporal trends that might otherwise be overlooked in models treating space and time separately. By combining Bayesian inference with bootstrap-based validation, this methodology provides a powerful and comprehensive analytical strategy for evaluating evolving processes over space and time. Such integration deepens understanding of the underlying phenomena while strengthening the reliability of findings, making it a valuable tool for research and decision-making in diverse fields where spatial and temporal dependencies are critical.

In summary, this introduction highlights the growing importance of Bayesian hierarchical frameworks for modelling longitudinal spatio-temporal data. The proposed integration of space-time interactions with bootstrap-based validation provides a coherent and robust methodology that addresses the limitations of conventional approaches. This combination advances the methodological framework available to researchers, ensuring both accurate parameter estimation and reliable inference. With increasing access to high-resolution spatio-temporal data, the role of robust Bayesian frameworks will only become more critical, supporting informed decision-making in epidemiology, environmental science, and other domains where dynamic processes unfold across both space and time.

2. Methodology

The Conditional Autoregressive (CAR) model is adopted as the core framework for Bayesian spatio-temporal analysis. The CAR model is widely recognized for its ability to capture spatial relationships by ensuring that neighboring regions influence one another, thereby reflecting the inherent dependence structures in areal data [4, 14]. Within the Bayesian paradigm, the CAR prior provides a natural way to incorporate prior knowledge and quantify uncertainty, while simultaneously smoothing spatial estimates to improve prediction reliability. Moreover, CAR models are computationally efficient, making them well-suited for large-scale datasets. Their flexibility in handling aggregated areal-level information, such as district- or state-level case reports, makes them particularly valuable in epidemiological studies, for example in mapping and analyzing measles outbreaks across regions.

Spatial and temporal autocorrelations (random effects) were modeled via the conditional autoregressive (CAR) model proposed by [17] and extended by [2] whose model can be expressed as

$$Y_{kt} | N_{kt}, \theta_{kt} \sim \text{Binomial}(N_{kt}, \theta_{kt}), \quad (1)$$

where

$$\log\left(\frac{\theta_{kt}}{1-\theta_{kt}}\right) = X_{kt}^T \beta + \phi_k + \delta_t + \gamma_{kt}. \quad (2)$$

The proposed model is decomposed into the spatio-temporal random effects with 3 components as follows: where ϕ_k is the spatial effect, δ_t is the temporal effect and γ_{kt} is the set of spatio-temporal auto correlation random effect for the community k and time period t. $\theta_{kt} = Y_{kt}/N_{kt}$ is the proportion of children that having measles in space k at time t, for $k = 1, \dots, k, t = 1, \dots, N$ where the $N_{kt} = 80, 160, 240, 320$ and 400 respectively β is a vector of regression coefficients corresponding to covariates X . After adjusting for covariate effects, the first component captures the overall spatial random effect common to all time period, represented by $\phi = (\phi_1, \phi_2, \dots, \phi_n)$. The spatial relationships between communities in this study were shown by binary neighborhood matrices W .

$$\phi_k | \phi_{-k}, W, \rho, \tau^2 \sim N \left(\frac{\rho_S \sum_{j=1}^k w_{kj} \phi_j}{\rho_S \sum_{j=1}^k w_{kj+1} - \rho_S}, \frac{\tau_S^2}{\rho_S \sum_{j=1}^k w_{kj+1} - \rho_S} \right). \quad (3)$$

The second part is a random effects in time that shows the overall trend in time that all communities share. This is shown by $\delta = (\delta_1, \delta_2, \dots, \delta_n)$

where
$$\delta_t | \delta_{-t}, D \sim N \left(\frac{\rho_T \sum_{j=1}^N d_{tj} \delta_j}{\rho_T \sum_{j=1}^N d_{tj+1} - \rho_T}, \frac{\tau_T^2}{\rho_T \sum_{j=1}^N d_{tj+1} - \rho_T} \right). \quad (4)$$

In this study, temporal relationships between dependent variable were determined using an adjacency weights matrix, a binary $N \times N$, where $N = 1, 2, \dots, N$ temporal neighborhood matrix. $D = d_{tj}$ where $d_{tj} = 1$ is defined if $|j - t| = 1$ and $d_{ij} = 0$ otherwise.

The model can also include an optional set of independent space-time interactions, which are shown by $\gamma = (\gamma_1, \gamma_2, \dots, \gamma_{nt})$ where $\gamma_{kt} \sim N(0, \tau_t^2)$. (5)

and

$$\tau_S^2, \tau_T^2, \tau_I^2 \sim \text{Inverse - Gamma}(1, 0.001)$$

where $\tau_S^2, \tau_T^2, \tau_I^2$ represents random effects that can happen in spatial, temporal, and space-time.

$\rho_S, \rho_T \sim \text{Uniform}(0, 1)$ and ρ_S and ρ_T are spatial dependence parameters and temporal dependence parameters that control how strong spatial and temporal autocorrelations are.

In the Bayesian spatio-temporal model, the interaction term (γ_{kt}) accounts for the combined influence of spatial and temporal dependencies. This term is crucial for accurately modeling data that exhibits both spatial and temporal correlations, such as infectious disease spread.

A Conditional Autoregressive (CAR) prior is used to model spatial dependencies, ensuring that neighboring regions influence each other. The interaction term follows a Gaussian CAR prior:

$$\gamma_{kt} | \gamma_{-kt} \sim N(\mu_{kt}, \sigma_{kt}^2),$$

where μ_{kt} represents the conditional mean given the neighboring spatial and temporal values, and σ_{kt}^2 is the conditional variance.

Spatial dependence is incorporated through a weighted sum of neighboring spatial effects:

$$\sum_{j=1}^k w_{kj} \phi_{k'} \quad (6)$$

where w_{kj} are the spatial weights defining the influence of neighboring location j on location k, and q_s controls the strength of spatial autocorrelation.

Temporal dependence is similarly modeled using a weighted sum of past interaction terms:

$$\sum_{j=1}^N d_{tj} \delta_k \quad (7)$$

where d_{tj} are temporal weights capturing dependencies across time points, and q_t reflects the persistence of temporal correlation.

The interaction term is then obtained by taking a weighted average of the spatial and temporal components:

$$\mu_{kt} = \frac{\rho_S \sum_{i=1}^k w_{kj} \phi_k + \rho_T \sum_{i=1}^N d_{tj} \delta_k}{\rho_S \sum_{i=1}^k w_{kj} + \rho_T \sum_{i=1}^N d_{tj}} \quad (8)$$

This formulation ensures that both spatial and temporal influences are normalized appropriately. The variance of the interaction term γ_{kt} is defined as:

$$\sigma_{\kappa\tau}^2 = \frac{\tau_t^2}{\rho_S \sum_{j=1}^k w_{kj} + \rho_T \sum_{j=1}^N d_{tj}}, \quad (9)$$

where τ^2 represents the variance parameter of the interaction effect.

Thus, the full distribution of the interaction term is:

$$\gamma_{kt} \mid \gamma - kt \sim N \left(\frac{\rho_S \sum_{i=1}^k w_{kj} \phi_k + \rho_T \sum_{i=1}^N d_{tj} \delta_k}{\rho_S \sum_{i=1}^k w_{kj} + \rho_T \sum_{i=1}^N d_{tj}}, \frac{\tau_t^2}{\rho_S \sum_{i=1}^k w_{kj} + \rho_T \sum_{i=1}^N d_{tj}} \right), \quad (10)$$

The interaction term, denoted as γ_{kt} , represents the effect at the location k and time t . The set of spatial neighbors for a given location k is represented by ϕ_k , while δ_t defines the set of temporal neighbors for time t . The spatial weights, w_{kj} , indicate the relationship between location k and its neighboring location j , whereas the temporal weights, d_{tj} , capture the influence over time t and its neighboring time s .

The variances associated with the spatial, temporal, and space-time interaction effects are assigned inverse-gamma priors: τ_s^2, τ_T^2 and $\tau_t^2 \sim \text{Inverse-Gamma}(1, 0.001)$.

These priors ensure flexibility while penalizing extreme variance estimates.

Finally, the spatial and temporal dependence parameters are assigned uniform priors:

The spatial and temporal dependence parameters are modeled as:

$\rho_S \rho_T \sim \text{Uniform}(0,1)$, and ρ_S and ρ_T spatial dependence parameters and temporal dependence parameters that control how strong spatial and temporal autocorrelations are.

2.1. Bootstrap Methodology

The bootstrap is a widely used resampling technique for assessing the variability of parameter estimates and constructing confidence intervals. Given an observed dataset $D = \{y_1, y_2, \dots, y_n\}$ with sample size n , and an estimator $\theta = T(D)$ of a parameter θ , the bootstrap procedure generates B resampled datasets $D^*_1, D^*_2, \dots, D^*_B$, each obtained by sampling with replacement from the original dataset. The bootstrap estimates are then computed as:

$$\theta^*_b = T(D^*_b), \text{ for } b = 1, 2, \dots, B$$

The empirical distribution of $\theta^*_1, \theta^*_2, \dots, \theta^*_B$ serves as an approximation to the sampling distribution of θ . Confidence intervals can be constructed from the percentiles of this distribution. For example, the 95% bootstrap confidence interval is given by:

$$[\theta^*(0.025), \theta^*(0.975)]$$

where $\theta^*(p)$ denotes the p^{th} quantile of the bootstrap distribution. This approach is especially advantageous when the theoretical distribution of the estimator is difficult to derive, or when the sample size is small and parametric approximations may not hold. The bootstrap has been widely used in longitudinal and spatio-temporal modelling to validate Bayesian posterior estimates and to provide complementary measures of uncertainty. Classical contributions include [18, 10], while more recent applications in Bayesian hierarchical modelling and spatio-temporal data include [7, 21, 1].

2.2. Simulation Study

We conducted a simulation study to quantify the ability of the developed model to correctly assemble areas based on their temporal trends, spatial trend and interaction trend using the Gibbs sampling approach.

Data were simulated using Binomial logistic model, the model consists of the data likelihood $Y_{kt} \sim \text{Binomial}(n, \theta_{kt})$ where

$$\log\left(\frac{\theta_{kt}}{1-\theta_{kt}}\right) = \beta_0 + \beta_1 x_{1kt} + \beta_2 x_{2kt} + \phi_k + \delta_t + \gamma_{kt} \tag{11}$$

x_{1kt}, x_{2kt} are normally distributed covariate with mean 0 and variance 1, $\phi_k, \delta_t, \gamma_{kt}$ corresponds to spatial and temporal that are drawn from multivariate normal distribution with mean vectors 0 and covariance structure defined as $\Sigma_K = 0.01Q_W^{-1}$, where W is the $K \times K$ distance matrix and $\Sigma_N = 0.01Q_D^{-1}$, where D is the $N \times N$ temporal matrix. The spatial-temporal covariance structures were simulated using

$$Q_W = 0.8\mathbf{I}_K \mathbf{1}'W - W + 0.2\mathbf{I}_K \mathbf{1} \tag{12}$$

for spatial effect

$$Q_D = 0.8\mathbf{I}_N \mathbf{1}'D - D + 0.2\mathbf{I}_N \mathbf{1} \tag{13}$$

for temporal effect.

This scheme implies that spatial and temporal correlations are set as $\rho_S, \rho_T = 0.8$ which also results in spatial, temporal and interaction effect defined by $\tau_S^2, \tau_T^2, \tau_I^2 = 0.2$. In addition, the intercept and covariate coefficients are defined as $\beta = (0, 0.5, 0.5)$ and $K = 16$ and $N = 5, 10, 15, 20$ and 25 areal units, $n_{kt} = N \times K = 80, 160, 240, 320$ and 400. Following, the simulation of the covariates and spatio-temporal effects and interaction, the response probability θ_{kt} were then simulated using

$$\theta_{kt} = \frac{\exp(\beta_0 + \beta_1 x_{1kt} + \beta_2 x_{2kt} + \phi_k + \delta_t + \gamma_{kt})}{1 + \exp(\beta_0 + \beta_1 x_{1kt} + \beta_2 x_{2kt} + \phi_k + \delta_t + \gamma_{kt})}. \tag{14}$$

The response variable Y_{kt} was then generated from the $\text{binomial}(n_{kt}, \theta_{kt})$ distribution. The next step involve the application of the newly developed R function "binomial.est" to simulate the posterior distribution. The posterior distribution for the proposed model was obtained from 10,000 MCMC independent samples, which were generated from a single Markov Chain that was run for 120,000 iterations with a 20,000 burn-in period, subsequently thinned by 10 to reduce the autocorrelation of the Markov chain convergence and monitored using graphically Geweke diagnostic.

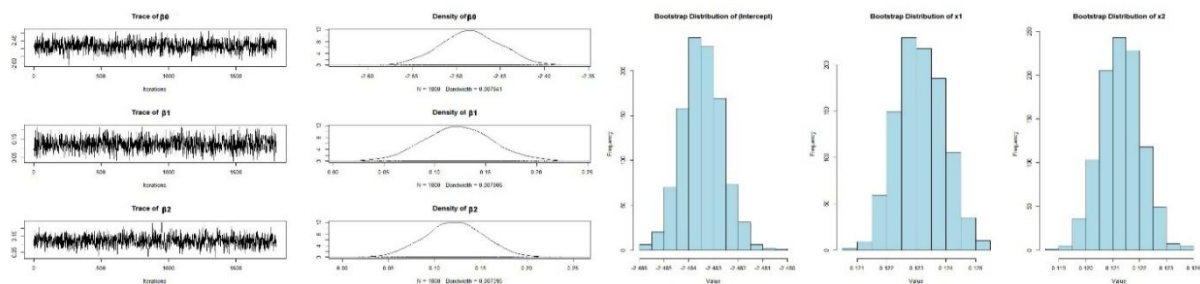


Figure 1: Convergence of the Markov chain and bootstrap distribution plots for the areal unit with $n_{kt}=80, K=16, n=5$ with true values $\beta_0 = 0, \beta_1 = 0.5, \beta_2 = 0.5$.

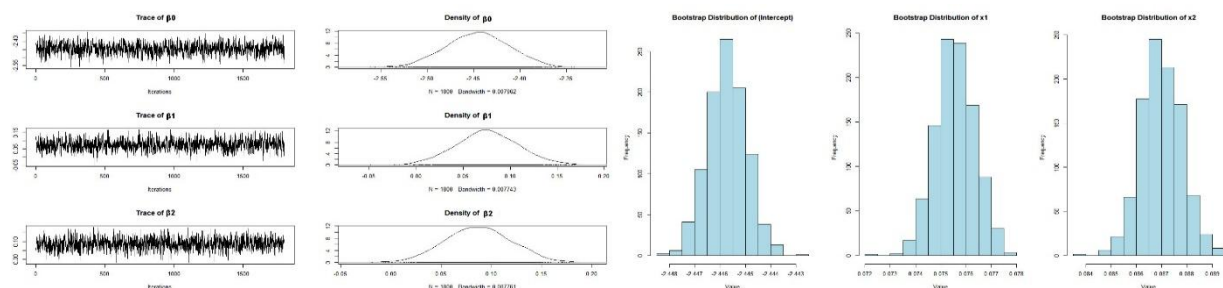


Figure 2: Convergence of the Markov chain and bootstrap distribution plots for the areal unit with $n_{kt}=160, K=16, n=10$ with true values $\beta_0 = 0, \beta_1 = 0.5, \beta_2 = 0.5$.

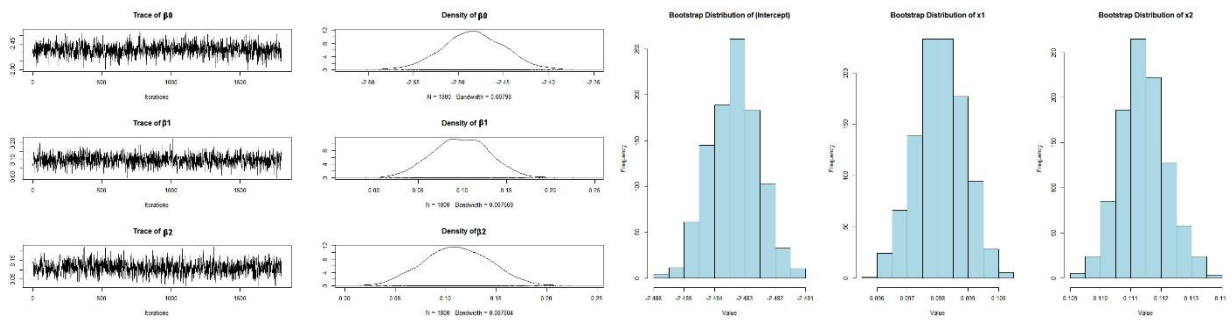


Figure 3: Convergence of the Markov chain and bootstrap distribution plots for the areal unit with $n_{kt}=240$, $K=16$, $n=15$ with true values $\beta_0 = 0, \beta_1 = 0.5, \beta_2 = 0.5$.

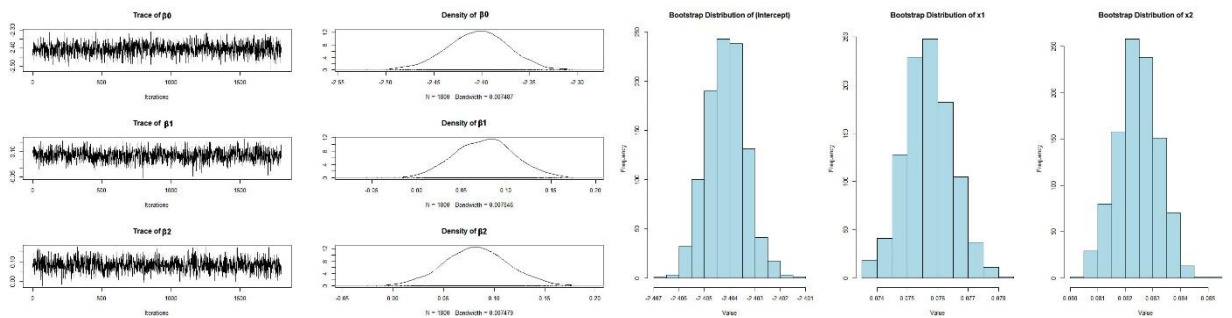


Figure 4: Convergence of the Markov chain and bootstrap distribution plots for the areal unit with $n_{kt}=320$, $K=16$, $n=20$ with true values $\beta_0 = 0, \beta_1 = 0.5, \beta_2 = 0.5$.

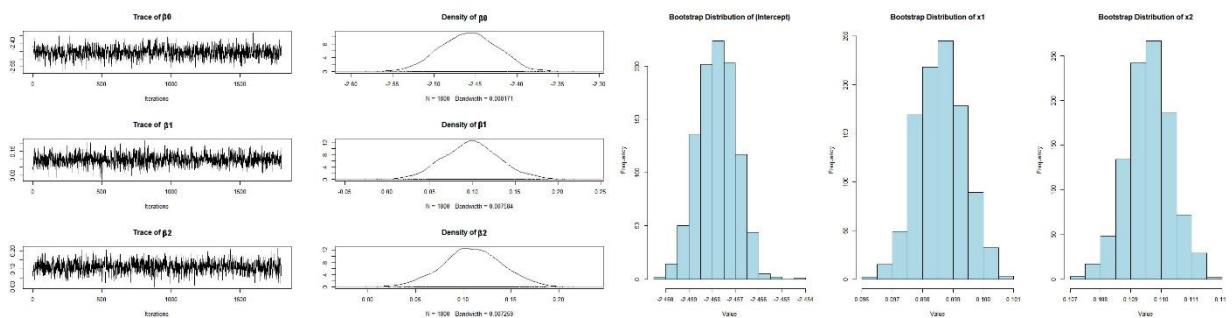


Figure 5: Convergence of the Markov chain and bootstrap distribution plots for the areal unit with $n_{kt}=400$, $K=16$, $n=25$ with true values $\beta_0 = 0, \beta_1 = 0.5, \beta_2 = 0.5$.

Figures 1 to 5 present convergence diagnostics and bootstrap distribution results for the estimated parameters β_0 , β_1 , and β_2 behave across different group sizes (80, 160, 240, 320, and 400). In each case, the number of regions (K) is fixed at 16, and the sample size increases from $n = 5, 10, 15, 20, 25$. The true values for the parameters are set as $\beta_0 = 0, \beta_1 = 0.5$, and $\beta_2 = 0.5$. The trace plots (left side of each figure) show how the parameter values change over time during the simulation. These plots look stable and show no major trend, which means the model is working well and the simulation has settled properly.

The bootstrap histograms shown in the right column of each figure further confirm the reliability of the estimates. Each distribution is unimodal and symmetric, centered around the posterior means, reinforcing the robustness of the Bayesian parameter estimates. As the areal unit size increases, the variation in bootstrap estimates decreases, illustrating greater precision in parameter estimation. These results collectively support that the model's performance improves with larger sample sizes and that the Bayesian approach used here effectively captures both the central tendencies and uncertainty of the parameters across different spatial aggregations.

Table 1: Posterior mean estimates and 95% credible intervals (C.I) for parameters $\beta_0, \beta_1, \beta_2, \tau_S, \tau_T, \tau_I, \rho_S$ and ρ_T across different areal units, $n_{kt} = N * K = 80, 160, 240, 320, 400$ with longitudinal value, $K = 16$, and sample size $N = 5, 10, 15, 20, 25$ and true parameter values $\beta_0 = 0, \beta_1 = 0.5, \beta_2 = 0.5$ and $\rho_S = \rho_T = 0.8$

Areal Unit n_{kt}	Parameter	Mean estimate	95% C.I	Bootstrap estimate	Confidence interval
80	β_0	-2.4864	(-2.5522, 2.4206)	-1.4398	(-1.4210, 1.4880)
	β_1	0.1228	(0.0562, 0.1887)	0.0941	(0.0931, 0.0962)
	β_2	0.0051	(0.0016, 0.0131)	0.1019	(0.1005, 0.1036)
	ρ_S	0.4486	(0.0267, 0.9245)	0.4760	(0.4644, 0.4882)
	ρ_T	0.3998	(0.0165, 0.9083)	0.3629	(0.3052, 0.4291)
	τ_S	0.0049	(0.0016, 0.0129)	0.0050	(0.4000, 0.0050)
	τ_T	0.0072	(0.0018, 0.0234)	0.0070	(0.0040, 0.0050)
	τ_I	0.0037	(0.0013, 0.0086)	0.0040	(0.0060, 0.0070)
160	β_0	1.5708	(1.4037, 1.6223)	1.2972	(1.2471, 1.4440)
	β_1	0.5675	(0.4583, 0.6726)	0.076	(0.0743, 0.0771)
	β_2	0.4822	(0.3773, 0.5842)	0.0871	(0.0853, 0.0891)
	ρ_S	0.4631	(0.0249, 0.9270)	0.4554	(0.4444, 0.4661)
	ρ_T	0.3597	(0.0165, 0.8728)	0.4053	(0.3924, 0.4171)
	τ_S	0.0108	(0.0024, 0.0361)	0.0050	(0.0050, 0.0060)
	τ_T	0.0093	(0.0019, 0.0325)	0.0070	(0.0060, 0.0070)
	τ_I	0.0620	(0.0028, 0.3209)	0.0040	(0.0040, 0.0050)
240	β_0	1.5570	(1.4536, 1.6702)	1.2093	(1.1485, 1.4923)
	β_1	0.5314	(0.4428, 0.6219)	0.0982	(0.0970, 0.1005)
	β_2	0.5165	(0.4281, 0.6092)	0.1112	(0.1106, 0.1139)
	ρ_S	0.4151	(0.0235, 0.9124)	0.4306	(0.4191, 0.4404)
	ρ_T	0.4200	(0.0194, 0.9038)	0.4358	(0.4254, 0.4506)
	τ_S	0.0158	(0.0021, 0.0768)	0.0050	(0.0050, 0.0060)
	τ_T	0.0088	(0.0020, 0.0276)	0.0070	(0.0060, 0.0070)
	τ_I	0.0310	(0.0159, 0.0542)	0.0040	(0.0040, 0.0050)
320	β_0	1.5344	(1.3893, 1.7163)	1.4408	(1.4060, 1.4182)
	β_1	0.5135	(0.4305, 0.6079)	0.0762	(0.0741, 0.0770)
	β_2	0.5021	(0.4198, 0.5931)	0.0821	(0.0813, 0.0845)
	ρ_S	0.4151	(0.0181, 0.9005)	0.4352	(0.4253, 0.4464)
	ρ_T	0.5523	(0.0429, 0.9619)	0.4203	(0.4082, 0.4328)
	τ_S	0.0078	(0.0020, 0.0262)	0.0050	(0.0050, 0.0060)
	τ_T	0.0233	(0.0040, 0.0708)	0.0070	(0.0060, 0.0070)
	τ_I	0.0206	(0.0073, 0.0584)	0.0040	(0.0040, 0.0050)
400	β_0	1.5623	(1.4580, 1.7575)	1.4005	(1.4591, 1.4664)
	β_1	0.5097	(0.4364, 0.5985)	0.0991	(0.0970, 0.1006)
	β_2	0.5544	(0.4792, 0.6419)	0.1103	(0.1081, 0.1119)
	ρ_S	0.4097	(0.0157, 0.9185)	0.4742	(0.4619, 0.4834)

ρ_T	0.3733	(0.0112, 0.8685)	0.4081	(0.3962, 0.4215)
τ_S	0.0131	(0.0022, 0.0451)	0.0050	(0.0050, 0.0060)
τ_T	0.0128	(0.0024, 0.0395)	0.0060	(0.0060, 0.0070)
τ_I	0.1900	(0.0142, 0.8984)	0.0030	(0.0030, 0.0040)

3. Results and Discussion

The relationship between the log-odds of θ_{kt} and the predictors was expressed as $\frac{\ln(\theta_{kt})}{1-\theta_{kt}} = \beta_0 + \beta_1 x_{1kt} + \beta_2 x_{2kt}$. The regression coefficients were specified as $\beta = (0, 0.5, 0.5)$.

To obtain the posterior distribution for our proposed model, we conducted Markov chain Monte Carlo (MCMC) sampling. 20,000 MCMC independent samples were generated from a single Markov chain and discarded the initial 2,000 samples as a burn-in period and thinned the remaining samples by 10 to reduce autocorrelation. Convergence of the MCMC chain was assessed using the Geweke diagnostic method, as well as graphical checking.

The analysis across different areal unit sizes ($n = 80, 160, 240, 320, 400$) demonstrates variations in the estimated parameters and correlation structures of the Bayesian spatio-temporal model with space-time interaction effects. At $n = 80$, the Intercept β_0 was negative, suggesting a lower baseline level of the response variable after accounting for covariates and random effects. As the areal unit size increased ($n = 160$ to 400), β_0 shifted to positive values, indicating a higher baseline effect. The 95% credible intervals narrowed slightly for larger n , reflecting improved precision in parameter estimation. Bootstrap estimates also followed similar trends, though they consistently differed in magnitude from the posterior means, showing the inherent methodological differences between Bayesian estimation and resampling approaches.

Both covariates β_1 and β_2 were positive across all areal units, implying that increases in these covariates were associated with increases in the response variable. Their magnitudes were generally larger in the Bayesian posterior means than in the bootstrap estimates, particularly at smaller areal units. As the areal unit size increased, the 95% credible intervals became narrower, reflecting greater stability and precision in parameter estimation at coarser spatial scales.

The spatial correlation (ρ_s) remained moderately positive, with posterior mean values ranging between approximately 0.41 and 0.46 across all areal units, indicating persistent spatial autocorrelation regardless of spatial resolution. The bootstrap estimates for ρ_s were comparable in magnitude, reinforcing the robustness of the model in capturing spatial dependencies. However, the Bayesian credible intervals were relatively wide, particularly at smaller areal units, reflecting greater uncertainty when fewer aggregated units were available. The temporal correlation (ρ_t) fluctuated between approximately 0.36 and 0.55 across areal units, with the highest values observed at $n = 320$, suggesting stronger temporal persistence at intermediate spatial aggregation. Although the bootstrap estimates for ρ_t were generally slightly lower, they followed a similar pattern to the Bayesian results. Notably, the credible intervals were wider for smaller areal units, reflecting greater uncertainty in temporal correlation estimates at finer spatial scales.

The variance components revealed distinct patterns across spatial scales. The spatial variance (τ_s) remained consistently small, indicating that only a limited portion of the overall variability was attributable to purely spatial effects. Similarly, the temporal variance (τ_t) was low across all areal units, suggesting minimal unexplained temporal fluctuations once covariates and spatial effects were incorporated. In contrast, the interaction variance (τ_i) displayed greater variability, particularly at smaller areal units, highlighting the presence of more localized and heterogeneous space-time interactions. Bootstrap estimates of these variance components were generally more stable, with narrower intervals compared to Bayesian posterior estimates,

underscoring methodological differences in uncertainty quantification.

A key finding is that the estimates of β_0 , β_1 , and β_2 are sensitive to spatial scale, with greater variability observed at smaller areal units. In contrast, the spatial (ρ_s) and temporal (ρ_t) correlations remain relatively stable across different scales, suggesting that spatial and temporal dependencies are less affected by aggregation. This stability indicates that correlation parameters are robust to changes in spatial resolution, whereas fixed effects are more sensitive to scale differences.

4. Conclusions

In this study, we extended Bayesian spatio-temporal models by incorporating space-time interaction effects and evaluated their performance across multiple areal unit sizes. The simulation results demonstrated that the model successfully captured both covariate influences and spatio-temporal dependencies. Covariate 1 (β_1) consistently showed a strong positive association with the response variable, while Covariate 2 (β_2) also retained a positive effect across all spatial scales. Notably, the intercept (β_0) shifted from negative at $n=80$ to positive at $n \geq 160$, highlighting the effect of spatial aggregation on baseline estimates.

The spatial (ρ_s) and temporal (ρ_t) correlations remained moderate and stable across scales, indicating that these parameters are strong and less affected by spatial resolution. However, the variance components, particularly the interaction term (τ_i), were more sensitive to areal unit size, suggesting that smaller units capture localized and heterogeneous space-time interactions, whereas larger units smooth out such variability.

Convergence diagnostics, including trace plots, confirmed the stability of MCMC chains, ensuring reliable posterior estimates. Moreover, the close alliance between Bayesian and bootstrap estimates further validated the robustness of the results, even though differences in magnitude were expected due to methodological disparity.

Additionally, the model demonstrated strong predictive and explanatory power, effectively characterizing the relationship between predictors and health outcomes in simulated spatio-temporal epidemiological data. These findings enhance our understanding of spatial and temporal disease dynamics, particularly in the context of infectious diseases such as measles. Importantly, the results offer a practical framework for public health planning by emphasizing the robustness of correlation structures across scales while drawing attention to the scale sensitivity of fixed effects. Such insights are crucial for determining appropriate spatial resolutions for disease surveillance and designing targeted intervention strategies in regions vulnerable to outbreaks.

Author contributions: Conceptualization, A.A. Mustapha; Methodology, H.S. Zulkafli; Writing original draft, A.A. Mustapha; Writing review and editing, J. Arasan; Data curation, M.A. Mustapha.

Funding: This research was supported by the Borno State Scholarships Board, under Reference Number GOV/BOS/115150. The author gratefully acknowledges this financial support, which made the successful completion of the study possible.

Acknowledgements: The author sincerely acknowledges the valuable guidance, constructive feedback, and academic support received throughout the development of this research. Appreciation is also extended to colleagues and reviewers whose insights contributed to improving the quality of the simulation study.

Conflict of Interest: The author declares no conflict of interest. All simulations, methodological developments, and interpretations were conducted independently and were not influenced by any funding body or third party.

References

- [1] Adeoye, A., Smith, R., & Green, T. (2025). Efficient Bayesian spatio-temporal outbreak detection with parsimonious seasonality. *Journal of Computational Statistics*, 33(2), 145-162.
- [2] Aswi, Tiro, M. A., & Rais, Z. (2022, December). Bayesian spatial conditional autoregressive (CAR) Leroux model of Covid-19 cases in Makassar, Indonesia. In *AIP Conference Proceedings* (Vol. 2662, No. 1, p. 020028). AIP Publishing LLC.
- [3] Banerjee, S., Carlin, B. P., & Gelfand, A. E. (2015). *Hierarchical Modeling and Analysis for Spatial Data* (2nd ed.). Chapman & Hall/CRC.
- [4] Banerjee, S., Wall, M. M., & Carlin, B. P. (2014). Adaptive Bayesian multivariate disease mapping with spatially varying coefficients. *Biometrics*, 70(3), 872–883.
- [5] Bernardinelli, L., Clayton, D., Pascutto, C., Montomoli, C., Ghislandi, M., & Songini, M. (1995). Bayesian analysis of space-time variation in disease risk. *Statistics in Medicine*, 14(21–22), 2433–2443.
- [6] Blangiardo, M., & Cameletti, M. (2022). *Spatial and Spatio-temporal Bayesian Models with R-INLA* (2nd ed.). Wiley.
- [7] Chen, R., Li, X., & Ghosh, J. (2022). Bootstrap approaches for hierarchical Bayesian models in functional data analysis. *Bayesian Analysis*, 17(4), 955-978.
- [8] Cressie, N., & Johannesson, G. (2008). Fixed rank kriging for very large spatial data sets. *Journal of the Royal Statistical Society: Series B*, 70(1), 209–226.
- [9] Cressie, N., & Wikle, C. K. (2011). *Statistics for Spatio-Temporal Data*. Wiley.
- [10] Davison, A. C., & Hinkley, D. V. (1997). *Bootstrap methods and their application* (No. 1). Cambridge university press.
- [11] Geweke, J. (1992). Evaluating the accuracy of sampling-based approaches to the calculation of posterior moments. In J. M. Bernardo et al. (Eds.), *Bayesian Statistics* (pp. 169–193). Oxford University Press.
- [12] Hefley, T. J., Hooten, M. B., Hanks, E. M., Russell, R. E., & Walsh, D. P. (2017). Dynamic spatio-temporal models for spatial data. *Spatial statistics*, 20, 206-220.
- [13] Jin, B., Wu, Y., Miao, B., Wang, X. L., & Guo, P. (2014). Bayesian spatiotemporal modeling for blending in situ observations with satellite precipitation estimates. *Journal of Geophysical Research: Atmospheres*, 119(4), 1806-1819.
- [14] Lawson, A. B. (2018). *Bayesian Disease Mapping: Hierarchical Modeling in Spatial Epidemiology* (3rd ed.). Chapman & Hall/CRC.
- [15] Lee, D. (2011). A comparison of conditional autoregressive models used in Bayesian disease mapping. *Spatial and Spatio-temporal Epidemiology*, 2(2), 79–89.
- [16] Lee, D., Rushworth, A., & Sahu, S. K. (2023). Bayesian modeling of spatio-temporal data. *Wiley Interdisciplinary Reviews: Computational Statistics*, 15(2), e1596.
- [17] Leroux, B. G., Lei, X., & Breslow, N. (2000). Estimation of disease rates in small areas: a new mixed model for spatial dependence. In *Statistical models in epidemiology, the environment, and clinical trials* (pp. 179-191). New York, NY: Springer New York.
- [18] Tibshirani, R. J., & Efron, B. (1993). An introduction to the bootstrap. *Monographs on statistics and applied probability*, 57(1), 1-436.
- [19] Wang, Y., Chen, X., & Xue, F. (2024). A review of Bayesian spatiotemporal models in spatial epidemiology. *ISPRS International Journal of Geo-Information*, 13(3), 97.
- [20] Wang, L., Zhou, M., & Zhang, H. (2024). Advances in Bayesian spatio-temporal disease mapping: Models, methods, and applications. *Spatial and Spatio-temporal Epidemiology*, 49, 100601.
- [21] Yin, J., Brown, P., & Lawson, A. B. (2023). Hierarchical Bayesian spatio-temporal models for small-area COVID-19 incidence and risk prediction. *BMC Medical Research Methodology*, 23(1), 112.



Disclaimer/Publisher's Note: The views, opinions, and content expressed in all articles are solely those of the respective author(s) and contributor(s) and do not necessarily reflect those of the JSSCI, its editors, or the publisher. JSSCI and its editorial team assume no responsibility for any harm or damage resulting from the use of information, methods, or products mentioned in the publication.